

Vacuum thermal evaporated $(\text{AsSe})_{1-x}(\text{AgI})_x$ films: studies by spectroscopic ellipsometry and atomic-force microscopy*

T. HINEVA*, A. SZEKERES^a, P. PETKOV, M. ANASTASESCU^b, M. GARTNER^b, K. SALAMON^c

Laboratory of Thin Films Technology, Department of Physics, University of Chemical Technology and Metallurgy, 8 Kl. Ohridsky blvd, 1756 Sofia, Bulgaria

^a*Institute of Solid State Physics, Bulgarian Academy of Sciences, 72 Tzarigradsko Chaussee Blvd., 1784 Sofia, Bulgaria.*

^b*Institute of Physical Chemistry, Spl Independentei 202, Bucharest 060021, Romania*

^c*Institute for Physics, Bijenicka cesta 46, 10000 Zagreb, Croatia*

Vacuum thermal evaporated $(\text{AsSe})_{1-x}(\text{AgI})_x$ films with different compositions ($x = 5, 15, 20$ and 30 mol %) have been studied by spectroscopic ellipsometry and atomic-force microscopy. The ellipsometric results have shown that the optical constants and optical band gap energy values vary with increasing AgI content in the films. Additional XRD measurements revealed that the films are amorphous with more ordered structures at larger x values. AFM images visualized that randomly distributed hillocks emerged from the smooth film surface yielding an rms roughness of $0.6\text{-}1.0$ nm with a tendency to increase with increasing AgI content.

(Received November 5, 2008; accepted December 15, 2008)

Keywords: Chalcogenide thin films, Optical properties, AFM imaging, Spectroscopic ellipsometry

1. Introduction

Chalcogenide glassy semiconductors possess disordered structures with flexible arrangements of the glassy network and the ability to change their optical, physicochemical, and photoelectric properties under illumination [1-4]. One of the most investigated chalcogenide glasses is the stoichiometric compound As_2Se_3 , while the non-stoichiometric glasses have received less attention. Due to their potential applications in infrared optics, optoelectronics, optical memories, waveguides, holography, bio and chemical sensors, $\text{As}_x\text{Se}_{1-x}$ glass structures have been intensively studied during recent decades [5].

On the other hand, the properties of vitreous ionic conductors are of fundamental and practical interest. Ag^+ ion-containing chalcogenide glasses are particularly attractive, because they possess a high conductivity that can reach 10^{-2} $\text{S}\cdot\text{cm}^{-1}$ at room temperature. As-Se based amorphous chalcogenides doped with AgI are known as superionic conducting glasses, and are promising materials for solid electrolytes, batteries etc.

Our research interest is focused on As-Se-AgI glasses, because such films possess numerous interesting features,

with potential uses as chemical or optical chalcogenide fiber sensors. In this work, we present results of spectroscopic ellipsometry (SE) and atomic-force microscopy (AFM) investigations of $(\text{AsSe})_{1-x}(\text{AgI})_x$ films, deposited by a vacuum thermal evaporation technique, in order to clarify some optical and surface properties as a function of film composition.

2. Experimental details

Thin films were deposited by standard thermal vacuum evaporation, using preliminarily synthesized bulk glasses with corresponding compositions [6]. The evaporation was performed in a Leybold LB 370 vacuum installation at a residual gas pressure of 1.33×10^{-4} Pa, using a suitable tantalum crucible. The experiments were carried out with a constant geometry of the experimental setup and evaporation temperatures in the range $850\text{-}1000$ K.

Ellipsometric measurements were performed with a Rudolf Research ellipsometer in a spectral region from 300 to 820 nm. The accuracy of the polarizer, analyzer and incidence angles was within $\pm 0.01^\circ$. The thicknesses of the

* Paper presented at the International School on Condensed Matter Physics, Varna, Bulgaria, September 2008

films and their optical parameters, i.e. the refractive index (N), extinction coefficient (k), absorption coefficient (α) and optical band gap energy (E_g), were evaluated from the SE data analysis. The accuracy of the film thickness was ± 0.2 nm, while that of the N and k values was ± 0.005 .

The AFM measurements were conducted in Dynamic Force Module/Intermittent contact mode, using an EasyScan 2 model from Nanosurf® AG Switzerland. The phase contrast working mode was used for the sample imaging, by means of a $10 \mu\text{m} \times 10 \mu\text{m}$ high resolution scanner on different scanning areas from $8 \mu\text{m}^2$ down to a sub-micron scale. Cantilevers with a typical force constant of 32 N/m, SiN tips with a curvature radius of 10 nm and a resonant frequency around 166 kHz were used.

Grazing incidence wide angle x-ray scattering (GIWAXS) measurements were performed using a modified laboratory SAXS/WAXS (small/wide angle x-ray scattering) experimental setup [7] adapted with a tilting specimen stage for grazing incidence. This asymmetric geometry under a pre-selected grazing incidence angle is particularly suitable for surface characterization and thin film structure analysis [8]. The GIWAXS spectra were acquired with a curved position sensitive detector (RADICON; 4096 pixels/55 deg), allowing the pattern to be collected in the 2θ range from 20° to 75° ; using $\text{Cu}_{K\alpha}$ radiation. The grazing incidence angle was about 1° for all samples; being large enough to allow the X-rays to penetrate throughout the whole films and small enough to reduce the substrate contribution.

3. Results and discussion

By solving the inverse problem of ellipsometry, the complex refractive index ($\tilde{N}=N-ik$) values were determined. The results are summarized in Fig. 1. The refractive index at $\lambda = 800$ nm and the thicknesses of the studied films are presented in Table 1.

In the literature, there are reports regarding the thickness dependence of the refractive index of As_2Se_3 films, showing a tendency to decrease with increasing film thickness [9]. A similar tendency can be expected in our case: the films have different compositions and thicknesses (Table 1) and the refractive index values will be affected by these two factors, i.e. by the composition and thickness. The simultaneous action of these factors results in an inconsistent refractive index variation and absence of a considerable compositional dependence, as can be seen in Fig. 1.

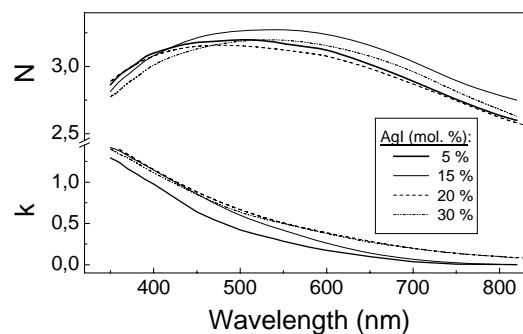


Fig. 1. Dispersion curves of the refractive index N and extinction coefficient k for different AgI contents in the deposited films.

The films are transparent in the near infrared region, as seen from the spectral dependence of the extinction coefficient in Fig. 1. Adding 20 and 30 mol. % AgI to AsSe results in an enhanced absorption with close k values.

Table 1. Refractive index at $\lambda = 800$ nm and thickness of the VTE $(\text{AsSe})_{1-x}(\text{AgI})_x$ films

| Composition | N at $\lambda = 800$ nm | Thickness, nm |
|---------------------------------------|-------------------------|---------------|
| $(\text{AsSe})_{95}(\text{AgI})_5$ | 2.64 | 720 |
| $(\text{AsSe})_{85}(\text{AgI})_{15}$ | 2.78 | 930 |
| $(\text{AsSe})_{80}(\text{AgI})_{20}$ | 2.61 | 1000 |
| $(\text{AsSe})_{70}(\text{AgI})_{30}$ | 2.67 | 840 |

From the dispersion curves of the extinction k , the absorption coefficient α has been calculated ($\alpha = 4\pi k/\lambda$) and the optical band gap energy values have been derived from Tauc plots of the relation $(\alpha h\nu)^{1/2}$ versus photon energy ($h\nu$) [10] by extrapolation of the linear part of the plot. The intercept of the line with the energy axis gives the E_g values. The dependence of the E_g on the silver iodide content is presented in Fig. 2.

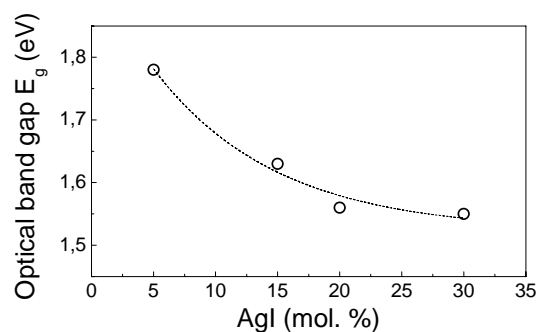


Fig. 2. Optical band gap energy in dependence of the AgI content in the $(\text{AsSe})_{1-x}(\text{AgI})_x$ films.

A gradual decrease of the optical gap from 1.78 to 1.55 eV has been observed when the AgI content in the films increases from 5 to 30 mol %. For a stoichiometric and 680 nm thick As_2Se_3 composition, the registered optical band gap is $E_g=1.75$ eV [9]. Various other values are given in the literature, for instance for a virgin $\text{As}_{40}\text{Se}_{60}$ film $E_g = 1.80$ eV [11], 1.76 eV [1], 1.793 eV [12] and for $\text{As}_{30}\text{Se}_{70}$ $E_g = 1.82$ eV [13]. Prieto-Alcón et al. [14] give a value of $E_g = 1.87$ eV for an as-evaporated $\text{As}_{50}\text{Se}_{50}$ film, and Sarsembinov et al. [15] report $E_g = 1.8$ eV for a thermally evaporated AsSe film. The E_g values reported in [16] for vacuum thermal evaporated As_2Se_3 films show an increase from 1.67 eV to 1.79 eV with the addition up to 35 mol % AgI. Our study on non-stoichiometric AsSe(AgI) films revealed a tendency for a decrease with increasing AgI addition (Fig. 2). The excess of As with respect to the selenium atoms, as well as the addition of AgI into the As-Se matrix, leads to an increase in the disorder and the formation of a more defective structure, responsible for an increase in the number of localized states in the band gap, and consequently to a decrease in the optical band gap energy. For the same reason, a higher AgI concentration in an As-Se glass results in a stronger absorption, but after 20 mol% AgI, probably a saturation of bonds and defects occurs and a further increase in the AgI concentration causes only a further weak decrease in the E_g value.

Additional information about the films' structure was gained from XRD measurements. The results are given in Fig. 3. There are no Bragg peaks related to a crystalline phase, and the spectra are typical of an amorphous material. The observed broad peak at around 30° becomes more intense and sharp for the highest concentration of AgI in the film, which could be connected with a more ordered film structure (Fig.3).

AFM investigation revealed an alteration of the surface morphology with changes in the AgI content. For a low AgI content (5 mol. %), randomly distributed hillocks emerging from the smooth film surface were visualized, which developed from grains (Fig. 4a and 4b). The surfaces of the films with higher AgI contents look smoother. However, periodic grooves formed on the surface were clearly seen (Fig. 4c). In films with 30 mol % AgI, on the perfectly smooth surface, parallel deep grooves with a well-pronounced periodicity were observed (Fig. 4d).

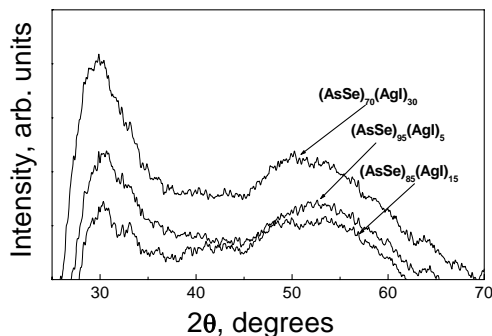
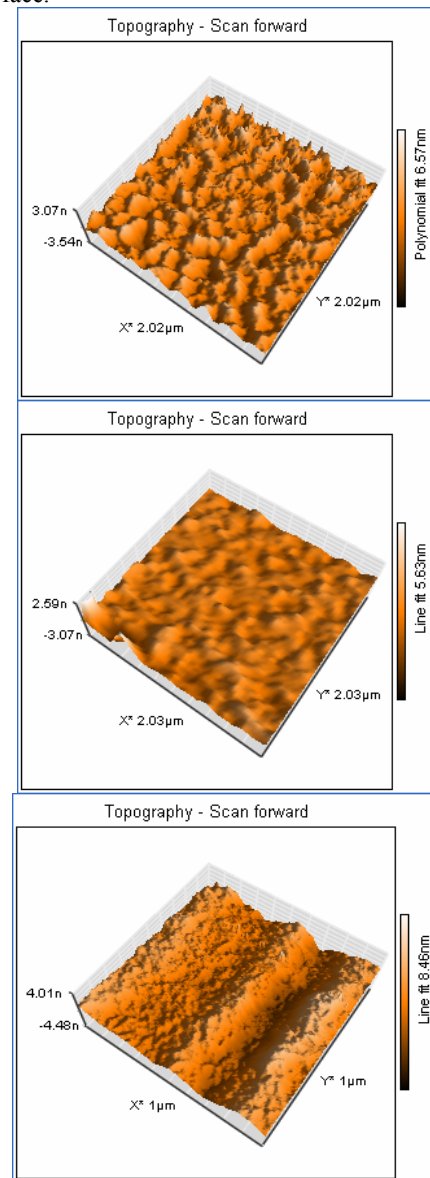


Fig. 3. Grazing incidence wide angle X-ray scattering of the $(\text{AsSe})_{1-x}(\text{AgI})_x$ vacuum thermally evaporated films ($x=5, 15, 30$ mol. %).

The ellipsometric (Figs. 1 and 2) and XRD (Fig. 3) measurements revealed that an increase in the AgI content in the films caused structural changes, reflected by grooves created at the film surface. As a result, the average surface roughness was enhanced with increasing AgI concentration in the film. This is illustrated in Fig. 5, where the root mean square (rms) roughness values, calculated over two different scanning areas, are presented. As seen, the rms values are 0.6 – 1.0 nm. The smaller scanning area is characterized by a higher surface roughness. The rms results are typical of a relatively flat film surface.



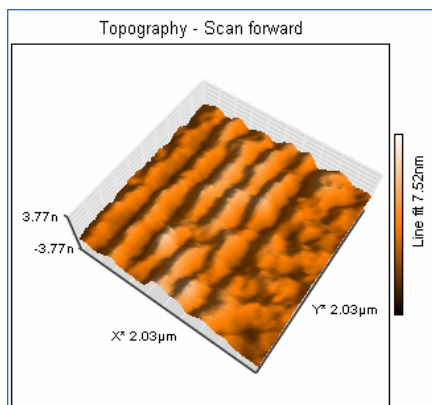


Fig. 4. AFM 3D images from the surface of vacuum evaporated $(AsSe)_{1-x}(AgI)_x$ films. The x value in the film composition varies, as follows: a) $x=5$; b) $x=15$; c) $x=20$ and d) $x=30$.

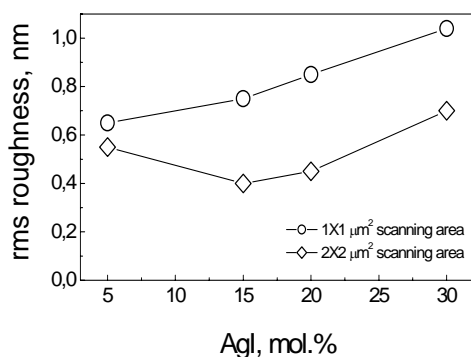


Fig. 5. Effect of the scanning area on the rms roughness of the $(AsSe)_{1-x}(AgI)_x$ film surfaces.

4. Conclusions

The presented results on the vacuum thermally evaporated $(AsSe)_{1-x}(AgI)_x$ films indicate that the refractive index and extinction coefficient values change with the AgI content, and the optical band gap values decrease with increasing AgI content. All films were amorphous, with more ordered structures in films with higher AgI contents. The AFM investigation revealed grains, emerging as hillocks from the smooth surface, and grooves growing parallel and with periodicity. As a whole, a very smooth film surface was grown, yielding a rms roughness of 0.6-1.0 nm with a tendency to increase with increasing AgI content.

Acknowledgements

The authors acknowledge with thanks the support of this work under the 2006-2008 Collaboration Agreement between the Bulgarian Academy of Sciences and the Romanian Academy of Sciences. T. Hineva and P. Petkov gratefully acknowledge the financial support of the National Science Fund under Grant No. VUF 1505.

References

- [1] J. Singh, K. Shimakawa, *Advances in Amorphous Semiconductors*, Taylor & Francis, London and New York (2003).
- [2] Y. Ikeda, K. Shimakawa, *Chalcogenide Letters* **2**, 127 (2005).
- [3] A. M. Andriesh, M. S. Iovu, S. D. Shutov, J. Optoelectron. Adv. Mater. **4**, 631 (2002).
- [4] G. Chen, H. Jain, M. Vlcek, A. Ganjoo, *Phys. Rev. B* **74**, 174203 (2006).
- [5] T. Gotoh, K. Tanaka, *J. Appl. Phys.* **89**, 4703 (2001).
- [6] T. Petkova, P. Petkov, P. Jóvári, I. Kaban, W. Hoyer, A. Schöps, A. Webb, B. Beuneu, *J. Non-Cryst. Solids* **353**, 2045 (2007).
- [7] O. Glatter, O. Kratky, *Small Angle X-ray Scattering*, Academic Press, New York, 1982.
- [8] M. Birkholz, *Thin Film Analysis by X-Ray Scattering*, Wiley, Weinheim, 2006.
- [9] D. C. Sati, R. Kumar, R.M. Mehra, *Turk. J. Phys.* **30**, 519 (2006).
- [10] N. F. Mott, E. A. Davis, *Electronic Processes in Non-Crystalline Materials*, Clarendon Press, Oxford, 1979.
- [11] J. B. Ramirez-Malo, E. Márquez, C. Corrales, P. Villares, R. Jiménez-Garay, *Mater. Sci. Eng., B* **25**, 53 (1994).
- [12] K. Antoine, H. Jain, N. Vlcek, *J. Non-Cryst. Solids* **352**, 595 (2006).
- [13] C. Corrales, Ph. D. thesis, University of Cádiz, 1994.
- [14] R. Prieto-Alcón, J. M. González-Leal, R. Jiménez-Garay, E. Márquez, *J. Optoelectron. Adv. Mater.* **3**, 287 (2001).
- [15] Sh. Sh. Sarsebinov, O. Yu. Prikhodko, A. P. Ryaguzov, S. Ya. Maksimova, *Semicond. Sci. Technol.* **16**, 872 (2001). PII: S0268-1242(01)26389-5.
- [16] T. Hineva, T. Petkova, C. Popov, P. Petkov, J. P. Reithmaier, T. Fuhrmann-Lieker, E. Axente, F. Sima, C. N. Mihailescu, G. Socol, I. N. Mihailescu, *J. Optoelectron. Adv. Mater.* **9**, 326 (2007).

*Corresponding author: thrhineva@yahoo.com